WM-98-114
JLAB-THY-98- 37

The Thomas Jefferson National Accelerator Facility

Theory Group Preprint Series

Additional copies are available from the authors.

The Southeastern Universities Research Association (SURA) operates the Thomas Jefferson National Accelerator Facility for the United States Department of Energy under contract DE-AC05-84ER40150

Relativistic theory of few body systems and their electromagnetic interactions*

Franz Gross
Department of Physics, College of William and Mary,
Williamsburg, Virginia 23185,
and Thomas Jefferson National Accelerator Facility,
12000 Jefferson Avenue, Newport News, VA 23606

Abstract

Recent results obtained from the manifestly covariant spectator theory are summarized. A recent unpublished best fit to NN scattering using 13 OBE parameters gives $\chi^2 = 2.25$ and a triton binding energy of -8.491 MeV. This agreement is possible because of the existence of off-shell coupling of the phenomenological, intermediate range effective scalar exchanges (both isoscalar and isovector). The previously published results for the deuteron form factors are reviewed, and new, preliminary results for electrodisintegration of the deuteron are presented.

*Invited talk presented at the Workshop on Electronuclear Physics with internal targets and the BLAST detector, May 28–30, 1998, MIT.

I. THEORETICAL INTRODUCTION

I will begin this talk by outlining some of the various relativistic methods that can be used to describe the few body system relativistically. The rest of the talk will describe the theory and applications of the relativistic spectator theory (a manifestly covariant method) to few body systems. I will describe fits to NN scattering using the OBE model, deuteron wave functions, calculations of the three body binding energy, and applications to both elastic and inelastic scattering of electrons from deuterons.

A. Why should few-body calculations be done relativistically?

In my opinion relativistic methods should be used whenever possible, but in some circumstances relativistic effects are particularly important and we really must include them. Relativistic methods are essential when we wish

- to study light quarks (with a mass of a few MeV) and to understand the origin of dynamical quark mass,
- to go beyond phenomenology and relate currents and interactions to underlying fields,
- to study reactions at relativistic energies where (for example) the recoil velocity of a deuteron scattered elastically by a virtual photon with $Q^2 = 4$ GeV^2 is close to 70% of the speed of light,
- to study magnetic moments and spin dependent effects which are often of relativistic origin, or constrained by relativity,
- to be precise, even at low energies, where (for example) the small nuclear binding energies are a delicate balance between huge kinetic and potential energy terms, which transform differently under relativistic transformations, and
- to eliminate one unnecessary approximation.

A decision to do calculations relativistically is only the first step. There are many relativistic methods to choose from and unfortunately these different methods have very different properties and use very different language. Sometimes experts from different "schools" are unable to compare their results easily. Your choice of method strongly influences your world view.

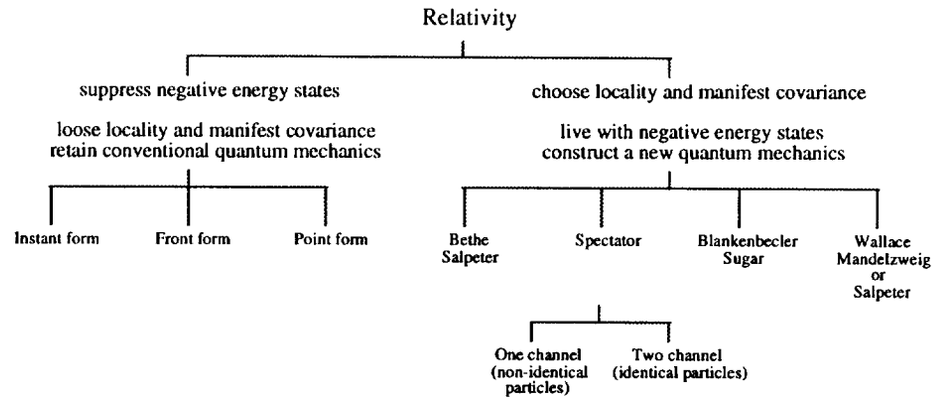

FIG. 1. The relativistic decision tree.

B. What relativistic method should be chosen?

Fig. 1 outlines these different approaches as a "decision tree". The first (and most profound) choice is between "Hamiltonian dynamics" (the left-hand branch) and "manifestly covariant dynamics" (on the right). If you use Hamiltonian dynamics you will be working with a conventional quantum mechanics in which the states span a Hilbert space with a positive definite norm. The infamous negative energy states are excluded from this space, and any effects from virtual negative energy intermediate states (the famous Z diagrams) must be put into the interactions or currents by hand. Since it uses conventional quantum mechanics, this method has the great advantage that the theoretical framework is well known and understood. Its only disadvantage is that some of the Lorentz transformations include the interaction, and therefore cannot be evaluated without doing additional dynamical calculations. For a review of this method see the article by Keister and Polyzou [1].

If you are willing to include negative energy states in your dynamics, it is possible to construct a formalism where *all* Lorentz transformations are "kinematic", i.e., they depend only on the momenta and spin of the particles and not on the interactions. In this case all Lorentz transformations (both rotations and boosts) can be carried out exactly, and all calculations are "manifestly covariant". This is a very nice way to handle relativity, but it has the disadvantage

that the unphysical negative energy states are part of your Hilbert space, and the theory is no longer a conventional quantum mechanics (for example, one encounters negative norm states when dealing with spin zero particles). This problem is not always apparent because these methods use field theory for guidance, but they are not strictly field theories and their systematic formulation is still under development.

These differences often lead to empty arguments at conferences. One theorist may assert that a state cannot be boosted exactly, while another will assert that the boosts *are* exact. The first theorist is correct if he is using Hamiltonian dynamics, and the second is correct if she is using manifestly covariant dynamics. Such profound differences in point of view make comparisons of practical calculations difficult.

As Fig. 1 illustrates, there are several different choices of method even within each of the broad approaches described above. In the context of Hamiltonian dynamics, one may use either the instant form, in which rotations are kinematic, or the front form, in which one boost is kinematic but rotational invariance is no longer independent of the dynamics. Similarly, there are several manifestly covariant approaches involving the use of different covariant equations. The studies by Fleisher and Tjon [2] use the famous Bethe-Salpeter equation, and there are equal time equations developed by Salpeter [3], Blankenbecler and Sugar [4] and Wallace and Mandelzweig [5]. In this talk I will describe results obtained with the spectator equation [6].

C. Properties of the spectator model

The spectator model has the following properties and features:

- All boosts and rotations are kinematic so that all Lorentz transformations can be evaluated *exactly*. Partial wave expansions can be used and all boosts are known.
- One of the nucleons in intermediate states is off-shell. This requires that it be described by both u (positive energy) and v (negative energy) spinors. For convenience, this degree of freedom is sometimes referred to as ρ-spin, with $\rho = +$ for positive energy states and $\rho = -$ for negative energies.
- In the description of NN scattering, the virtual contributions from negative ρ-spin states produce a strong repulsion at short distances sufficient to explain much of the repulsive core, and also make important contributions to the spin dependent parts of the interaction.

- When applying the spectator equations to the n-body system, $n-1$ particles are on-shell and only one particle is off-shell. When treating identical particles the progagator must be explicitly symmetrized, so that there are configurations in which any one of the n particles is off-shell.
- Total energy is conserved (in addition to the three-momentum) and this restriction together with the mass shell constraints reduces the number of continuous degrees of freedom to $3(n-1)$, as in nonrelativistic physics.
- If one of the particle masses goes to infinity, the two body equation reduces to a relativistic equation for the light particle moving in an instantaneous potential created by the heavy particle. This is referred to as the "one body limit", and it assures a smooth nonrelativistic limit with a simple physical interpretation. In this limit there are also some cancellations between ladders and crossed ladders to all orders. For theories involving scalar exchange, this cancellation is exact and one boson exchange (OBE) gives the exact result in the one body limit.
- The theory permits a close connection to field theory, so that electroweak currents are constrained by the dynamics.
- The explicit symmetrization required for identical particles may lead to kernels with spurious singularities.

All of these features are very desirable except for the last. Fortunately, these spurious singularities do not introduce singularities in any physical observables and their numerical effect is rather small. They may be removed by making small changes in the definitions of the kernels, so they are more a nuisance that a serious problem. Still, they are an unesthetic feature of this approach and it would be useful to find a way to eliminate them from the start. This is currently under investigation.

II. NN SCATTERING AND PROPERTIES OF OBE MODELS

The spectator equation for NN scattering is shown diagramatically in Fig. 2 and for the bound state (deuteron) in Fig. 3. It can be shown that the bound state equation follows automatically from the scattering equation without any additional assumptions. The kernels for the two equations are identical, and must be explicitly symmetrized to satisfy the Pauli principle. As discussed above, one of the two particles in on-shell, which means mathematically that its propagator is replaced by a delta function and an on-shell projection operator:

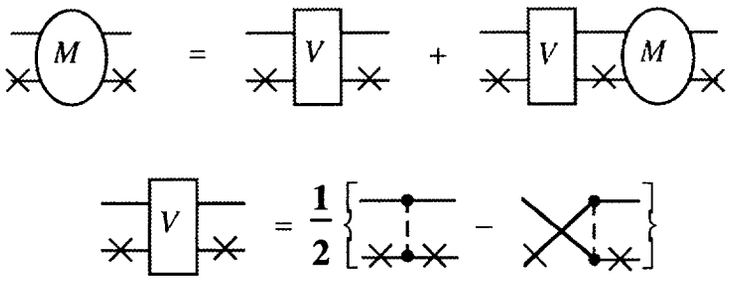

FIG. 2. Diagramatic representation of the spectator equations for NN scattering with an OBE kernel. For identical particles the kernel must be explicitly antisymmetrized. The $\times$ symbolizes that the particle is on-shell.

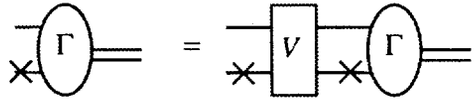

FIG. 3. Diagramatic representation of the spectator equations for the deuteron vertex function. The kernel is identical to the one shown in Fig. 2, and the equations can be derived from the scattering equation without additional assumptions.

particle	spin/ parity	isospin	mass	$g^2/4\pi$	off-shell parameter	κ_v	form factor mass	# of parms
π	0^-	1	134.98	13.34	0	–	$\Lambda_\pi \sim$ **2000**	1
η	0^-	0	548.8	**3.0 ± 0.25**	0	–	$\Lambda_\eta \sim$ **1300**	2
σ	0^+	0	**∼ 500**	**5.0 ± 0.5**	ν_σ	–	$= \Lambda_\eta$	2
δ	0^+	1	**∼ 500**	**0.6 ± 0.4**	ν_δ	–	$= \Lambda_\eta$	2
ω	1^-	0	782.8	**15.0 ± 1.0**	1.0	**∼ 0.2**	$= \Lambda_\eta$	2
ρ	1^-	1	760.0	**0.8 ± 0.2**	**1.55 ± 0.4**	**7.0 ± 0.5**	$= \Lambda_\eta$	3
N	$\frac{1}{2}^+$	$\frac{1}{2}$	936.8	–	–	–	$\Lambda_N \sim$ **1800**	1

TABLE I. OBE parameters. The 13 shown in bold face were varied during the fits. A family of models with $\nu_\sigma = -0.75\,\nu$ and $\nu_\delta = 2.6\,\nu$ are discussed in the text.

OBE para	IIB (rev.)	W00	W05	W10	W15	**W16**	W18	W19	W20	W22	W26
ν	0	0.0	0.5	1.0	1.5	1.6	1.8	1.9	2.0	2.2	2.6
G_π	13.15	13.34	13.34	13.34	13.34	13.34	13.34	13.34	13.34	13.34	13.34
G_η	3.023	3.350	2.714	2.455	2.849	2.969	3.193	3.322	3.437	3.639	3.949
G_σ	5.30275	5.84067	5.59454	5.50753	5.09315	4.99887	4.80199	4.67948	4.56381	4.36852	4.05718
m_σ	522	525	519	515	507	506	503	501	499	496	491
ν_σ	0.0	0.0	-0.375	-0.75	-1.125	-1.2	-1.35	-1.425	-1.5	-1.65	-1.95
G_δ	0.33136	0.14812	0.34622	0.69046	0.68120	0.62818	0.52659	0.47598	0.43276	0.35656	0.25045
m_δ	484	390	472	540	524	512	488	474	462	439	399
ν_δ	0.0	0.0	1.3	2.6	3.9	4.16	4.68	4.94	5.2	5.72	6.76
G_ω	10.087	12.801	13.430	14.767	15.028	14.879	14.617	14.439	14.267	13.932	13.361
κ_ω	0.095	0.207	0.150	0.119	0.177	0.195	0.227	0.247	0.264	0.298	0.356
G_ρ	0.443	0.561	0.645	0.807	0.901	0.899	0.878	0.870	0.852	0.814	0.733
κ_ρ	6.651	6.929	6.661	6.245	6.210	6.267	6.441	6.516	6.628	6.872	7.418
λ_ρ	0.863	1.533	1.499	1.520	1.553	1.556	1.557	1.559	1.558	1.555	1.548
Λ_π	2034	2304	2235	2203	2106	2075	2027	1992	1972	1935	1883
Λ_η	2034	1473	1394	1283	1213	1206	1195	1189	1185	1178	1165
Λ_N	1725	1629	1690	1759	1813	1822	1837	1847	1854	1867	1887
χ^2	2.53	3.00	2.71	2.45	2.26	**2.25**	2.26	2.27	2.31	2.44	2.56
$-E_T$	∼ 6.0	6.217	6.706	7.412	8.301	**8.491**	8.871	9.074	9.266	9.662	10.535
D/S	0.0247	0.0252	0.0253	0.0254	0.0255	0.0255	0.0255	0.0255	0.0255	0.0255	0.0255
P_{il}	5.0	5.3	5.6	6.0	6.4	6.4	6.5	6.5	6.6	6.6	6.7
P_{v_t}	0.048	0.015	0.011	0.005	0.002	0.002	0.002	0.002	0.002	0.002	0.003
P_{v_s}	0.009	0.007	0.003	0.001	0.001	0.001	0.002	0.002	0.002	0.003	0.004
$\langle V' \rangle$	2.0	2.6	1.6	0.3	-1.0	-1.2	-1.6	-1.7	-1.9	-2.2	-2.8

TABLE II. Deuteron properties and OBE parameters for the models discussed in the text. The couplings are all dimensionless, with $G_\pi = g_\pi^2/4\pi$, and E_T is in MeV. The χ^2 is for the 1994 np data set up to 350 MeV. The last four rows are *probabilities*.

$$\frac{m+\not{p}}{m^2-p^2-i\epsilon} \to 2\pi i\,\delta_+(m^2-p^2)\,(m+\not{p})\,. \tag{2.1}$$

A. New ν dependent fits to the NN data

The spectator equation with a one boson exchange (OBE) kernel has been used to fit the NN phases shifts successfully [7,8]. Six boson exchanges are used, as summarized in Table I. The detailed values of the parameters are given in Table II. The masses of the two effective "bosons" σ and δ and the form factor masses are varied during the fit. The remaining parameters are couplings defined as follows:

$$
\begin{aligned}
g_{\rm ps}\Lambda_{\rm ps}(p',p) &= g_{\rm ps}\left\{\gamma_5 - \frac{1-\lambda_{\rm ps}}{2m}\left[(m- \not{p}')\,\gamma_5 + \gamma_5\,(m- \not{p})\right]\cdots\right\} \\
&= g_{\rm ps}\left\{\lambda_{\rm ps}\,\gamma_5 + \frac{1-\lambda_{\rm ps}}{2m}\,\gamma_5\,\not{q}\cdots\right\} \\
g_{\rm s}\Lambda_{\rm s}(p',p) &= g_{\rm s}\left\{1 - \frac{\nu_{\rm s}}{2m}\left[m- \not{p}' + m- \not{p}\right]\cdots\right\} \\
g_{\rm v}\Lambda^{\mu}_{\rm v}(p',p) &= g_{\rm v}\left\{\gamma^{\mu} - \frac{\kappa_{\rm v}}{2m}i\sigma^{\mu\nu}q_{\nu} + \frac{\kappa_{\rm v}(1-\lambda_{\rm v})}{2m}\left[(m-\not{P}')\,\gamma^{\mu} + \gamma^{\mu}\,(m-\not{P})\right]\cdots\right\} \\
&= g_{\rm v}\left\{[1+\kappa_{\rm v}(1-\lambda_{\rm v})]\gamma^{\mu} - \frac{\kappa_{\rm v}\lambda_{\rm v}}{2m}i\sigma^{\mu\nu}q_{\nu} - \frac{(1-\lambda_{\rm v})\kappa_{\rm v}}{2m}P^{\mu}\cdots\right\} \qquad (2.2)
\end{aligned}
$$

The $\kappa_{\rm v}$ are the familiar f/g ratios for vector mesons, and, for historical reasons, the off-shell parameters are denoted by λ for the pseudoscalar and vector mesons, and by ν for the scalar mesons, and Eq. (2.2) shows that they are all proportional to the off-shell nucleon projection operators. They allow for the possibility of an independent coupling to the negative energy states. The family shown in Table II all have $\nu_\sigma = -0.75\,\nu$ and $\nu_\delta = 2.6\,\nu$. In all cases $\lambda_\pi = \lambda_\eta = 1$ and ν is fixed as shown. In the fit IIB, the pion coupling G_π was varied, but the constraint $\Lambda_\pi = \Lambda_\eta$ was imposed, leaving 13 free parameters. For the other fits G_π was fixed at 13.34, a value in agreement with the latest analyses, but Λ_π and Λ_η were free to vary independently, so these models also have 13 free parameters.

Please note that these results for the W family of models were just obtained a week before the completion of this report, and are not the same as the ones reported to the Workshop, or summarized in Ref. [8]. They were obtained after our minimization routine was corrected, and they produce significantly better fits to the two-body data. We now also have a spectacular prediction for the three body binding energy as will be reported below.

B. Deuteron wave functions

The mathematical connection between the covariant deuteron wave function, Ψ, and the dNN vertex with one N off-shell was developed many years ago [9]:

$$
\begin{aligned}
\Psi_{\alpha,\lambda}(P,p) &= \frac{1}{\sqrt{2M_d(2\pi)^3}}\,S_{\alpha\beta}(P-p)\,[\Gamma(P,p)C]_{\beta\gamma}\,\overline{u}^{T}_{\gamma}(\mathbf{p},\lambda) \\
&= \psi^{+}_{\lambda'\lambda}(\mathbf{P},\mathbf{p})\,u_{\alpha}(\mathbf{P}-\mathbf{p},\lambda') + \psi^{-}_{\lambda'\lambda}(\mathbf{P},\mathbf{p})\,v_{\alpha}(\mathbf{p}-\mathbf{P},\lambda')
\end{aligned}
$$

where S is the nucleon propagator, C is the Dirac charge conjugation matrix, and $u(\mathbf{p},\lambda)$ are Dirac spinors with three-momentum $\mathbf{p}$ and spin projection λ. In

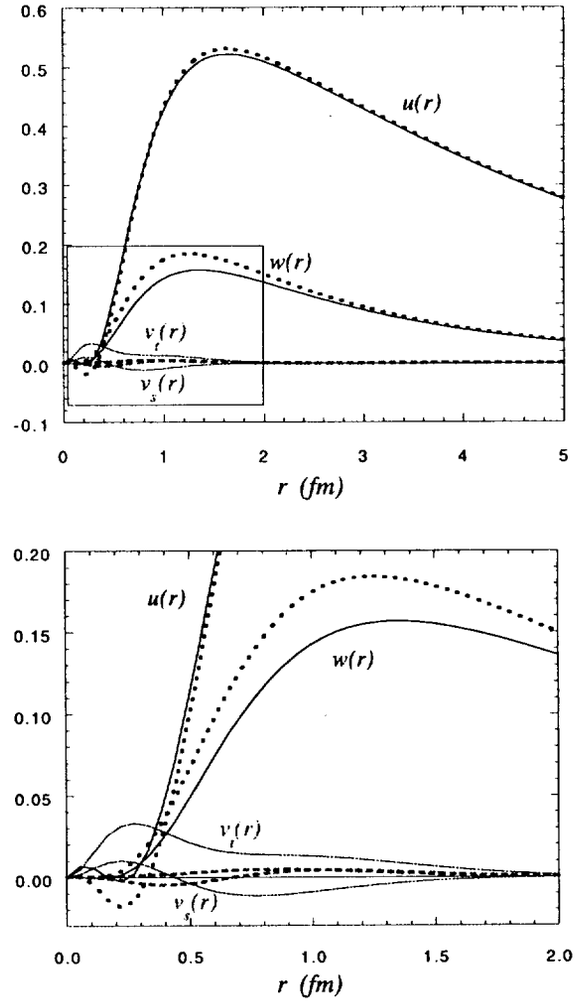

FIG. 4. The four relativistic wave functions for models IIB (solid lines) and W16 (dotted lines). The boxed region in the upper panel is shown in the lower panel.

the deuteron rest frame the nucleon propagator for the off-shell particle 2 can be expanded in terms of the spinors $u(-\mathbf{p},\lambda')$ and $v(\mathbf{p},\lambda')$, reflecting the separation of the propagator into a sum of terms with positive and negative energy poles. Then the relativistic wave function can be expressed in terms of four scalar wave functions, two required for ψ^+ and two for ψ^-

$$\psi^+_{\lambda'\lambda}(\mathbf{0},\mathbf{p}) = \frac{m}{\sqrt{2M_d(2\pi)^3}}\frac{\overline{u}(-\mathbf{p},\lambda')\Gamma(P,p)C\overline{u}^T(\mathbf{p},\lambda)}{E_p(2E_p - M_d)}$$
$$= \frac{1}{\sqrt{4\pi}}\left[u(p)\sigma_1\cdot\sigma_2 - \frac{w(p)}{\sqrt{8}}\left(3\sigma_1\cdot\hat{p}\,\sigma_2\cdot\hat{p} - \sigma_1\cdot\sigma_2\right)\right]\chi_{1M}$$
$$\psi^-_{\lambda'\lambda}(\mathbf{0},\mathbf{p}) = -\frac{m}{\sqrt{2M_d(2\pi)^3}}\frac{\overline{v}(\mathbf{p},\lambda')\Gamma(P,p)C\overline{u}^T(\mathbf{p},\lambda)}{E_pM_d}$$
$$= -\sqrt{\frac{3}{4\pi}}\left[v_s(p)\frac{1}{2}\left(\sigma_1-\sigma_2\right)\cdot\hat{p} + \frac{v_t(p)}{\sqrt{8}}\left(\sigma_1+\sigma_2\right)\cdot\hat{p}\right]\chi_{1M}$$

The functions u and w are the familiar S and D-state wave functions, while v_t and v_s are the spin triplet and singlet P-state wave functions. The normalization condition satisfied by these wave functions is

$$1 = \int_0^\infty p^2dp\left\{u^2 + w^2 + v_t^2 + v_s^2\right\} + \langle\frac{\partial V}{\partial M_d}\rangle\,, \tag{2.3}$$

where $\langle\partial V/\partial M_d\rangle$ is a term arising from the energy dependence of the kernel (see Ref. [7]).

The four wave functions, u, w, v_t, and v_s are shown in Fig. 4 for the two models of greatest interest: Model IIB for which successful results for the deuteron form factors have been obtained, and model W16 which gives the best fit to the two-body data and the three-body binding energy.

III. COVARIANT CALCULATION OF THE THREE BODY WAVE FUNCTION

The three-body spectator equations restrict two of the three particles to their mass shell [10,11]. This fixes both of the relative energies covariantly and leaves equations that depend on only two three-momentum variables, as in the nonrelativistic case. The resulting equations have a Faddeev-like structure as illustrated in Fig. 5. The two-body amplitudes that drive the equations are precisely the ones calculated from the two-body equations (shown in Fig. 2). There are *no*

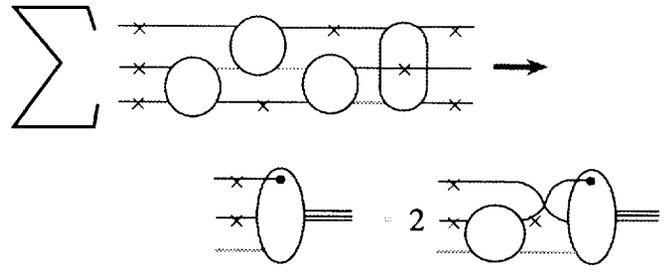

FIG. 5. Diagramatic representation of the summation of all two body interactions for three-body scattering, which leads to the three-body bound state equation for the triton. The amplitudes are properly anti-symmetrized and two of the three particles (labeled with an $\times$) are on-shell.

new parameters and the triton binding energy can be predicted uniquely from any two-body force model.

However, to obtain the three-body solutions the two-body amplitudes must be boosted from the overall three-body rest frame to the *two-body* rest frame where they were originally calculated. The size of this boost depends on the three momentum of the third non-interacting particle (the spectator). Because the spectator momentum is one of the internal integration variables, an exact covariant solution cannot be obtained unless we know how to boost the two-body amplitude to *any* velocity, and one of the real advantages of the spectator formalism is that this is both possible and practical [12].

Model IIB [7] which has been found to give an excellent description of the deuteron form factors (as shown below [13]) was found to give much too small a result; the binding energy was in the vicinity of -6.0 MeV, much less that the experimental result of -8.48 MeV. This model has no off-shell σ or δ couplings. After considerable study it was found that the binding energy could be improved by allowing the the off-shell parameters ν_σ and ν_δ to be non-zero. We found [8] that scaling ν_σ and ν_δ by the relations

$$\nu_\sigma = -0.75\,\nu$$
$$\nu_\delta = 2.6\,\nu\,,$$

and varying ν from 0 to 2.6 gives a triton binding energy that varies smoothly from about -6.0 MeV (for $\nu = 0$) to -10.0 MeV (for the largest $\nu = 2.6$). In each case *all other parameters*, except the pion coupling constant and the masses of the non-scalar mesons, *were varied to give the best fit to the two body data* before the three body binding energy was calculated. These results were originally published in Ref. [8].

Recently (at the end of August after this talk was given), I discovered that the fits originally published [8] were not optimal; there was an error in our minimization code which did not allow the best fit to be found. *New results for all the models*, denoted by Wn where n= $10\,\nu$, were obtained, and these results together with the original results for Model IIB are given in Table II. Note that some of the meson parameters (especially g_δ, g_ω, and g_ρ) are sensitive to the value of ν, while others (including the scalar meson masses, the cutoff masses, and κ_ρ) are less sensitive. All of the new models give an excellent value for the deuteron D/S ratio, and varying percentages for the D and P state probabilities. Note that the derivative term in the normalization condition (2.3), $\langle V' \rangle = \langle \partial V / \partial M_d \rangle$, varies significantly with ν. Alfred Stadler recalculated the trition binding energies for these models, and the variation of the triton binding energy for this family of models is shown graphically in the upper panel of Fig. 6. This variation is qualitatively similar to the result we published [8], but *all of the χ^2 are lower and the new minimum is very close to $\nu = 1.6$* instead of in the region $\nu \sim 1.8 - 1.9$ as originally published. Furthermore, the *new binding energies are slightly smaller* than those of Ref. [8]. Note the remarkable feature of the new results: *the same value of $\nu = 1.6$ gives the best triton binding energy and also the best two body fit.*

I conclude this section by noting that the relativistic calculations presented here include mechanisms which would be regarded as three-body forces in a non-relativistic context. These include single Z diagram contributions which arise from the negative energy part of the propagation of the off-shell nucleon. They also include contributions from the off-shell couplings outlined in Table II. For example, consider the sequential interaction of two σ mesons on one nucleon line. We could have the sequence of interactions:

$$-\frac{g_\sigma\,\nu_\sigma}{2m}\,(m - \not{p})\left(\frac{1}{m - \not{p}}\right) g_\sigma = -\frac{g_\sigma^2 \nu_\sigma}{2m}\,. \tag{3.1}$$

In this example the coupling of two sigmas collapses to a single four-point $\sigma\sigma NN$ contact interaction. In a similar fashion, off-shell couplings can induce contact interactions of arbitrarily large order involving any of the mesons in the OBE model. We conclude that *an OBE model with off-shell couplings is equivalent to another OBE model with no off-shell couplings but with multiple meson exchange contributions which induce three body forces.* It is clear that off-shell couplings provide a way to include many body forces.

IV. ELECTROMAGNETIC CURRENT OPERATOR

In the OBE models discussed above, the effective propagator for the off-shell nucleon is

$$\tilde{S}(p) = \frac{h^2(p^2)}{m - \not{p}} = \frac{h^2}{\Lambda_-(p)} \tag{4.1}$$

where $h = h(p^2)$ is the strong nucleon form factor. This propagator can be used in the presence of electromagnetic interactions if we introduce a reduced electromagnetic nucleon current operator j_r^μ. Current will be conserved in the general case if the reduced nucleon electromagnetic current operator satisfies the Ward-Takahashi identity

$$q_\mu j_r^\mu(p', p) = \left\{ \tilde{S}^{-1}(p) - \tilde{S}^{-1}(p') \right\}, \tag{4.2}$$

where we use the convention that the charge e is omitted from the definition of the current.

A current which satisfies this condition can be determined phenomenologically using the method of Gross and Riska [14]. Dropping terms proportional to $q^\mu = p'^\mu - p^\mu$, one choice for the off-shell current is

$$j^\mu(p', p) = F_0 \left\{ F_1 \gamma^\mu + F_2 \frac{i\,\sigma^{\mu\nu} q_\nu}{2m} \right\} + G_0 F_3\, \Lambda_-(p') \gamma^\mu \Lambda_-(p) \tag{4.3}$$

where F_3 is taken to be equal to $G_E(Q^2)$, F_1 and $F_2(Q^2)$ are the usual nucleon on-shell form factors, and

$$\begin{aligned} F_0 &= \frac{1}{h'^2}\,\frac{m^2 - p'^2}{p^2 - p'^2} + \frac{1}{h^2}\,\frac{m^2 - p^2}{p'^2 - p^2} \\ G_0 &= \left(\frac{1}{h'^2} - \frac{1}{h^2} \right) \frac{4m^2}{p'^2 - p^2}\,, \end{aligned} \tag{4.4}$$

with $h' = h(p'^2)$. When the final nucleon is on shell, $p'^2 = m^2$ and $h' = 1$, and the current reduces to

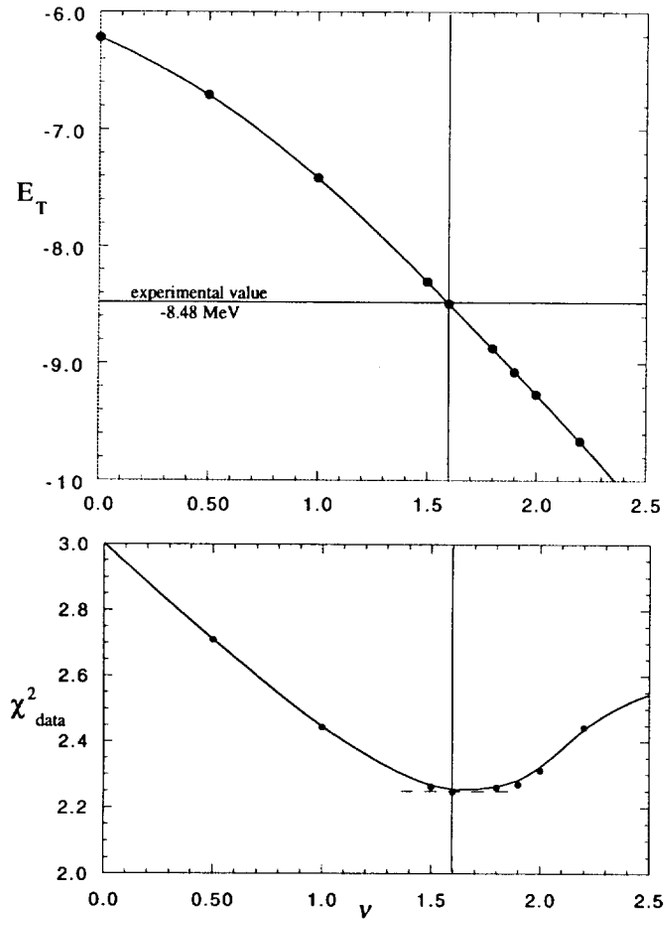

FIG. 6. The three body binding energy, E_T, and χ^2 for the fit to the two body data as a function of the off-shell mixing parameter ν. The solid dots are the data from Table II fitted by the smooth curves shown in the figures. The value $\nu = 1.6$ is marked by the vertical line and the short dashed line in the lower panel shows that the minimum χ^2 is very near $\nu = 1.6$.

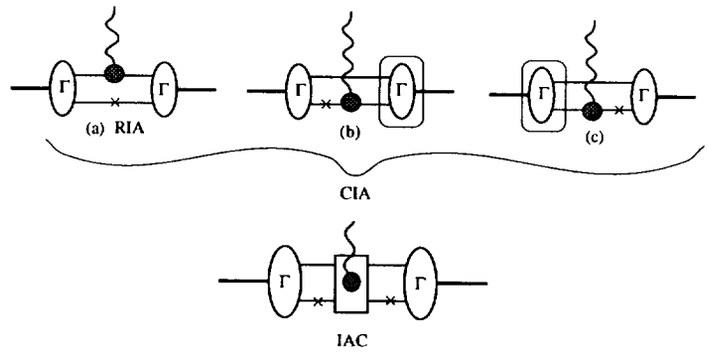

FIG. 7. Feynman diagrams that give the exact result of the deuteron form factors when the hadron interaction is described by an OBE model. As before, the × denotes particles which are on-shell.

$$j^{\mu}(p',p) = \left(F_1\gamma^{\mu} + F_2\frac{i\,\sigma^{\mu\nu}q_{\nu}}{2m}\right)\frac{1}{h^2}\,. \tag{4.5}$$

If both nucleons are on shell, $h = 1$ and it reduces to the usual result. The current (4.3) was used in the calculations reported below.

V. DEUTERON FORM FACTORS

Calculation of the deuteron form factors requires the evaluation of the four diagrams shown in Fig. 7. The top three diagrams are the complete impulse approximation (CIA) and the last is the interaction current (IAC) contribution. The two diagrams (b) and (c) each have singularities, but their sum is finite and, for identical particles, well approximated by the contribution from diagram (a), so the CIA can be approximated by 2 × diagram (a). If, in addition, the off-shell single nucleon current (4.3) is replaced by its on-shell form, this approximation is referred to as the relativistic impulse approximation (RIA), and this was used in earlier calculations [15].

Some recent results [13] for the deuteron structure functions obtained using Model IIB are shown in Figs. 8 and 9. Here I show A, B, and T_{20} defined by

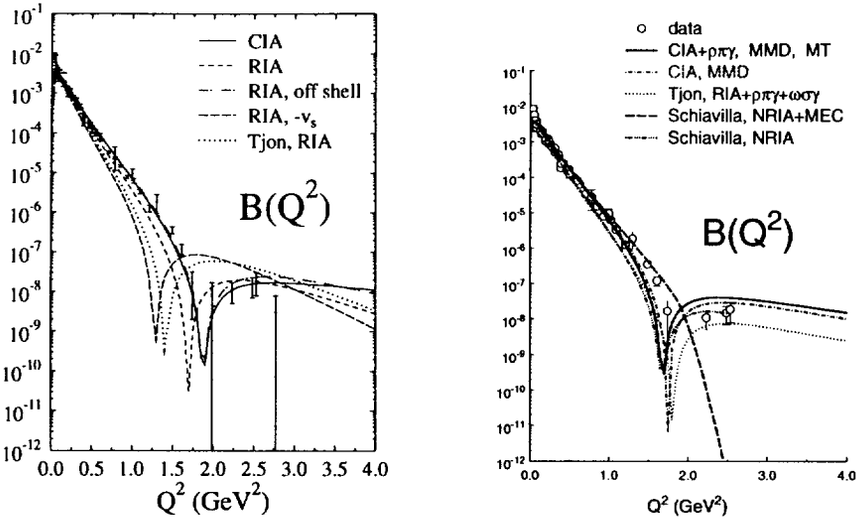

FIG. 8. The B structure function for Model IIB. Left panel: The CIA contribution discussed in the text. Right panel: The full calculations (including exchange currents) for various models discussed in the text.

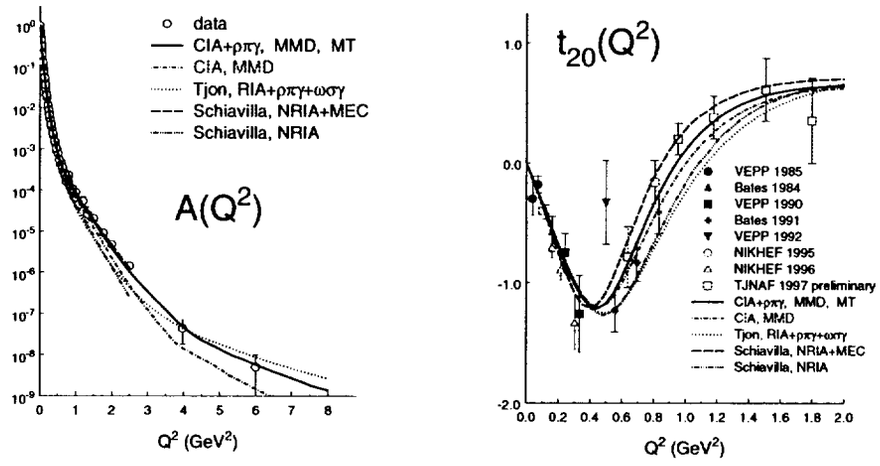

FIG. 9. The left panel shows A and the right panel T_{20} for the cases shown in Fig. 8.

$$A(Q^2) = G_C^2(Q^2) + \frac{2}{3}\eta\, G_M^2(Q^2) + \frac{8}{9}\eta^2\, G_Q^2(Q^2)$$

$$B(Q^2) = \frac{4}{3}\eta(1+\eta)\, G_M^2(Q^2)$$

$$T_{20}(Q^2) = -\sqrt{2}\frac{4}{3}\eta\, \frac{G_C(Q^2)G_Q(Q^2) + \frac{1}{3}\eta\, G_Q^2(Q^2)}{G_C^2(Q^2) + \frac{8}{9}\eta^2\, G_Q^2(Q^2)}$$

where $\eta = Q^2/(4M_d^2)$ and G_C, G_M, and G_Q are the charge, magnetic, and quadrupole form factors of the deuteron [15].

The B structure function turns out to be very sensitive to the details of the dynamics. The left panel of Fig. 8 compares our CIA calculation of B with various RIA approximations, including the one of Hummel and Tjon (HT) [16]. Note that our CIA gives a very good description of the data, leaving very little room for exchange currents. The major numerical difference between the new CIA (solid line) and the old RIA (short dashed line) is the use of the off-shell current operator; if the off-shell operator is used in the RIA (dashed-dotted line) it is indistinguishable from the CIA over the entire region of Q^2. The remaining difference between our RIA and the HT result is due to the small relativistic P-state components included in our calculation. If we change the sign of the small component, v_s, the RIA (labeled RIA, $-v_s$ in the figure) is not very different from the HT result, and far from the data.

This last observation is very surprising, because the probability of the v_s state is only 0.009%! The reason such a small component can have such a large effect is illustrated in Fig. 10. The effect is due to a "double" interference between the small P states and the larger S and D-state components. The magnetic form factor can be decomposed into electric and magnetic parts,

$$G_M(Q^2) = G_{Es}(Q^2)\, D_M^E(Q^2) + G_{Ms}(Q^2)\, D_M^M(Q^2)$$

where G_{Es} and G_{Ms} are the isoscalar electric and magnetic form factors of the nucleon. Expanding the body form factors to order $(v/c)^2$ gives

$$D_M^M(Q^2) = \int_0^\infty dr \left\{ [2u^2(r) - w^2(r)]\, j_0(\tau) + [\sqrt{2}u(r)w(r) + w^2(r)]\, j_2(\tau) \right\}$$

$$D_M^E(Q^2) = \int_0^\infty dr \left\{ \frac{3}{2}w^2(r) + \frac{2}{\sqrt{3}}mr \left(v_t(r) \left[\frac{1}{\sqrt{2}}u(r) - w(r) \right] - v_s(r) \left[u(r) + \frac{1}{\sqrt{2}}w(r) \right] \right) \right\} [j_0(\tau) + j_2(\tau)]\,,$$

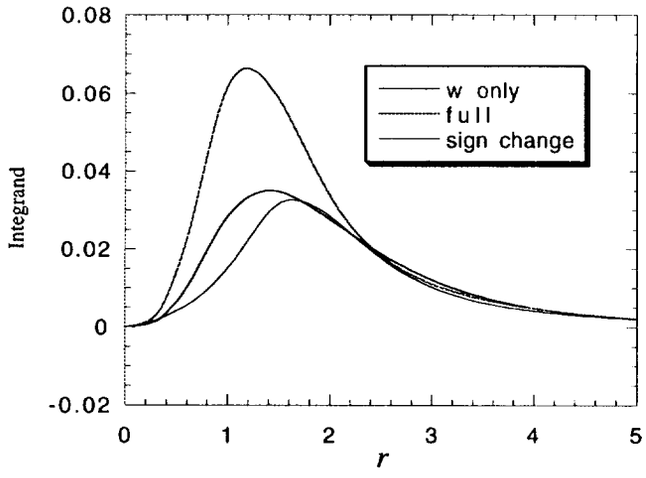

FIG. 10. The integrand of $D_M^E(0)$.

where $\tau = Qr/2$ [15]. Note the additional terms in D_M^E where the small components of the deuteron wave function interfere with the large components, enhancing the overall effect of the small components. A "second" interference will occur of the sign of the v_t component is opposite to v_s. In this case the two separate interference terms, which are individually small, will add coherently giving the large effect. This is the case for Model IIB, where the effect of this double interference is shown in Fig. 10. In this figure the curve with the large peak at ~0.07 is the integrand of $D_M^E(Q^2)$ (when $Q = 0$), while the curves with the smaller peaks are the w^2 term only and the integrand with the sign of v_s changed. The figure shows that, due to the double interference, a larger value of $D_M^E(Q^2)$ is obtained at the critical value of Q^2 when the leading term $D_M^M(Q^2)$ is small, accounting for the large shift in the position of the minimum. In is interesting that the same term gives a relativistic correction to the deuteron magnetic moment sufficient to give the correct value when the D state probability is 7% [17]:

$$\Delta\mu_d = \frac{2}{\sqrt{3}} m \int_0^\infty r dr \left\{ v_t(r) \left[\frac{1}{\sqrt{2}} u(r) - w(r) \right] - v_s(r) \left[u(r) + \frac{1}{\sqrt{2}} w(r) \right] \right\} .$$

The right panel of Fig. 8 and the two panels of Fig. 9 show that the results for all three structure functions when exchange currents are included. The curves labeled "CIA + $\rho\pi\gamma$" are our full calculation using the nucleon form factors of Mergell, Meissner, and Drechsel [18] and including the $\rho\pi\gamma$ exchange current evaluated with a $\rho\pi\gamma$ form factor calculated by Mitchell and Tandy [19]. Note

that this gives only a small contribution to the B and T_{20} observables, but that its contribution to A is larger. Unfortunately, until the neutron charge form factor is known, we are unable to draw definitive conclusions from A. The figures also show the calculations of Hummel and Tjon [16], who used large form factors for the $\rho\pi\gamma$ exchange current (see the discussion in Ref. [20]) and also included an $\omega\sigma\gamma$ exchange current, and Schiavilla and Riska [21], who use a nonrelativistic model with exchange currents and relativistic corrections to lowest order.

Our study of the deuteron from factors leads to the following conclusions:

- In the neighborhood of the zero the B structure function is very sensitive to the small relativistic P-state components of the deuteron wave function. This is a surprising result.
- There is evidence for the existence of small isoscalar $\rho\pi\gamma$ exchange currents, but no evidence for other interaction currents (except the Z diagram contributions which are not interaction currents in the covariant formalism).
- These observations would have been impossible without the use of a covariant model.

However, before we can draw definitive conclusions about the physics of the deuteron form factors, we must examine the results predicted by the models with non-zero values of ν. These models tend to have very tiny P-states, but also generate a new family of isoscalar exchange currents arising from the energy dependence of the off-shell couplings proportional to ν. It remains to be seen whether or not these new exchange currents will play the role played previously by the P-states.

VI. INELASTIC SCATTERING FROM THE DEUTERON

Electrodisintegration of the deuteron and the three body bound states has been studied extensively by many groups (see, for example, Tjon [22]). Recently, Arenhövel, Beck, and Wilbois [23] have pointed out that the relativistic effects in inelastic scattering can be very large. In this section I will report on some very recent work by Adam, Ulmer, Van Orden, and me [24] which confirms the observations made in Ref. [23] and by others. This work is preliminary and will be followed by more extensive calculations in the near future.

Fig. 11 shows the kinematics for the process $e + d \rightarrow e' + p + n$ (we use the notation of Ref. [25]). The coincidence unpolarized scattering cross section depends on four *covariant* structure functions

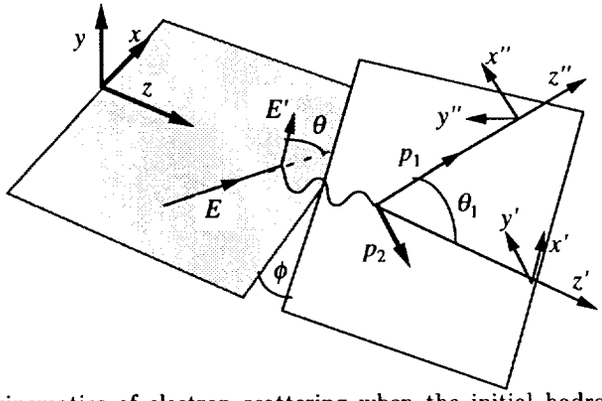

FIG. 11. The kinematics of electron scattering when the initial hadronic state is broken into two fragments with momenta p_1 and p_2.

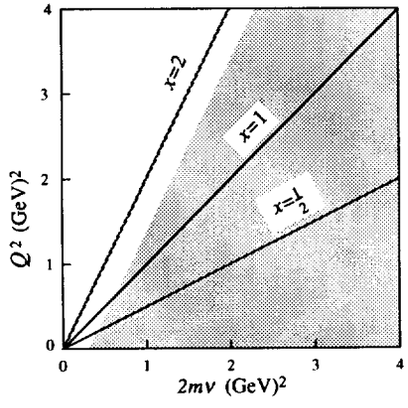

FIG. 12. The region of the ν–Q^2 plane accessible to electron scattering.

$$\frac{d^5\sigma}{d\Omega' dE' d\Sigma} = \frac{\sigma_M}{4\pi M_d}\frac{Q^2}{\mathbf{q}_L^2}\left\{\tilde{R}_L + s_T\tilde{R}_T - \frac{1}{2}\cos 2\phi\ \tilde{R}_{TT} + s_{LT}\cos\phi\ \tilde{R}_{LT}\right\}$$

where the kinematic factors are

$$s_T = \frac{1}{2} + \xi^2$$
$$s_{LT} = -\frac{1}{\sqrt{2}}\left(1+\xi^2\right)^{\frac{1}{2}}$$
$$\xi = \frac{|\mathbf{q}_L|}{Q}\tan\frac{\theta}{2},$$

with θ the electron scattering angle and ϕ the out-of-plane angle, as shown in Fig. 11.

The structure functions are related to the helicity matrix elements of the current

$$\tilde{R}_L = R_{00}$$
$$\tilde{R}_T = R_{++} + R_{--}$$
$$\tilde{R}_{TT} = 2\mathrm{Re}\ R_{+-}$$
$$\tilde{R}_{LT} = 2\mathrm{Re}\ (R_{0+} - R_{0-})$$

where (for unpolarized targets) the R's are

$$R_{\lambda_\gamma\lambda'_\gamma} = \frac{m^2}{\pi^2 W}\sum_{\lambda_1\lambda_1\lambda_d}\left\langle\lambda_1\lambda_2\left|J_{\lambda_\gamma}(q)\right|\lambda_d\right\rangle\left\langle\lambda_1\lambda_2\left|J_{\lambda'_\gamma}(q)\right|\lambda_d\right\rangle^*.$$

These structure functions depend on three variables: Q^2, ν, and the angle θ_1 between $\mathbf{p}_1$ and $\mathbf{q}$, where $\mathbf{p}_1$ is the three-momentum of the particle detected in coincidence with the final electron. It is convenient to specify θ_1 in the cm frame of the outgoing pair, where it always varies between 0 and π, regardless of the values of Q^2 and ν. The region of allowed values of Q^2 and ν is shown in Fig. 12. If the scattering is elastic, so that the deuteron remains bound after the scattering, the Bjorken variable $x = Q^2/2m\nu = 2$, and this defines one boundary of the allowed scattering region. As long as x remains close to 2, the final state remains below the pion production threshold up to very large values of Q^2, and one may try to explain the large Q^2 behavior of these inelastic processes using a theory with no pion rescattering in the final state.

The four unpolarized structure functions are only a small fraction of the structure functions which can be measured. With *polarized* electrons, targets, and recoiling nucleons many more can be studied [25,26], but these observables tend to

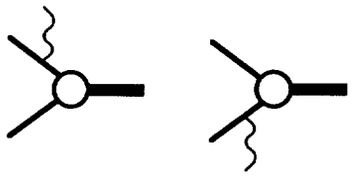

FIG. 13. The covariant plane wave Born approximation to deuteron electrodisintegration. Note that the *dnp* vertex functions used in these diagrams always have one particle on shell.

be very sensitive to final state interactions and interaction currents. The calculations presented here are obtained only from the pole diagrams shown in Fig. 13, and hence I limit discussion to the four unpolarized structure functions. After final state interactions and interaction currents have been included, we will be able to discuss the polarization observables.

Fig. 14 shows that the pole approximation does an excellent job of explaining the 180° SLAC data. It also shows that the relativistic effects are very large. Most of the relativistic effects seem to come from the corrections to the current, and there is no sensitivity to the different model wave functions (we compared the results from model IIB and the Paris model, as relativized in Ref. [23]).

Even the low energy Bernheim data [27] shown in Fig. 15 are well fit by the pole terms provided the lowest order v/c relativistic contributions are retained. In this case there is no evidence for relativistic effects of higher order in v/c, nor for model dependencies coming from the difference between the Paris and Model IIB wave functions. However, under more extreme (but still measurable conditions) the calculations show great sensitivity to all effects. This is illustrated in Figs. 16 and 17, which show the differential cross section, the ϕ asymmetry

$$A_\phi = \frac{d\sigma(\phi = 180°) - d\sigma(\phi = 0°)}{d\sigma(\phi = 180°) + d\sigma(\phi = 0°)}$$

and the four structure functions. The four curves show (i) the v/c approximation, (ii) the exact contribution for Model IIB, (iii) the exact contribution for the Paris wave function [23], and (iv) the result for Model IIB with the P-states set to zero. We see that the results are sensitive to all of these differences, and there are indications that these effects are measurably large [24]. Final conclusions await further analysis and the calculations of the final state and interaction current

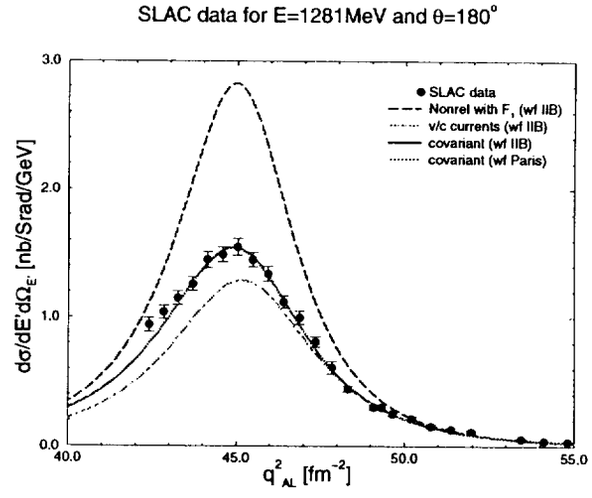

FIG. 14. Comparison of the covariant impulse approximation with the nonrelativistic and v/c approximations.

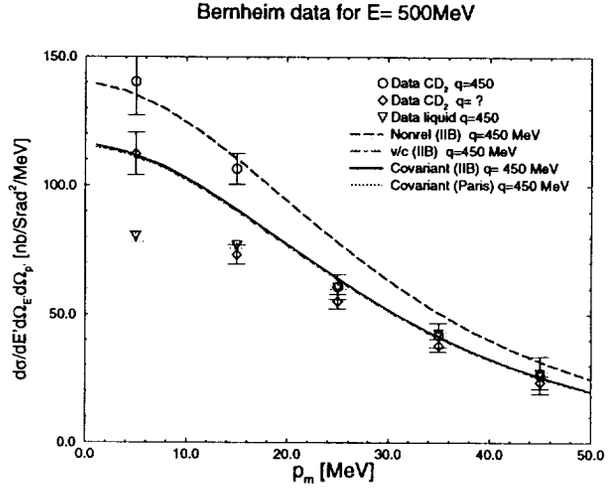

FIG. 15. The Bernheim data at low missing momentum. Note that the relativistic effects (mostly from the current operator) are significant.

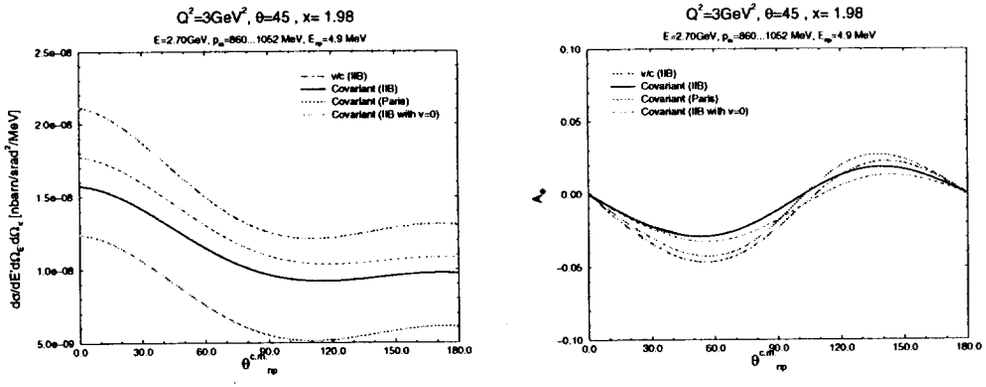

FIG. 16. The asymmetry factor A_ϕ and the differential cross section at "large" Q^2 and small W. Note that both are sensitive to *all* effects.

contributions, which could mask these effects.

VII. CONCLUSIONS

The relativistic theory in the few body sector is mature. The theory

- is consistent, fully developed, and gives a good description of the data,
- is successful in describing the deuteron (but we need to know G_{En}),
- shows that relativistic effects, particularly from the current operator, are important for inelastic scattering,
- has produced covariant three-body bound state wave functions which can be normalized.

The major theoretical tasks for the near future are to

- complete the covariant calculations of all spin dependent observables for $d(e,ep)n$ for final states with small mass, and look for measurable observables which are sensitive to short range dynamics, and
- begin covariant calculation of the ^{3}H and ^{3}He form factors and look at electrodisintegration of the three-nucleon bound states.

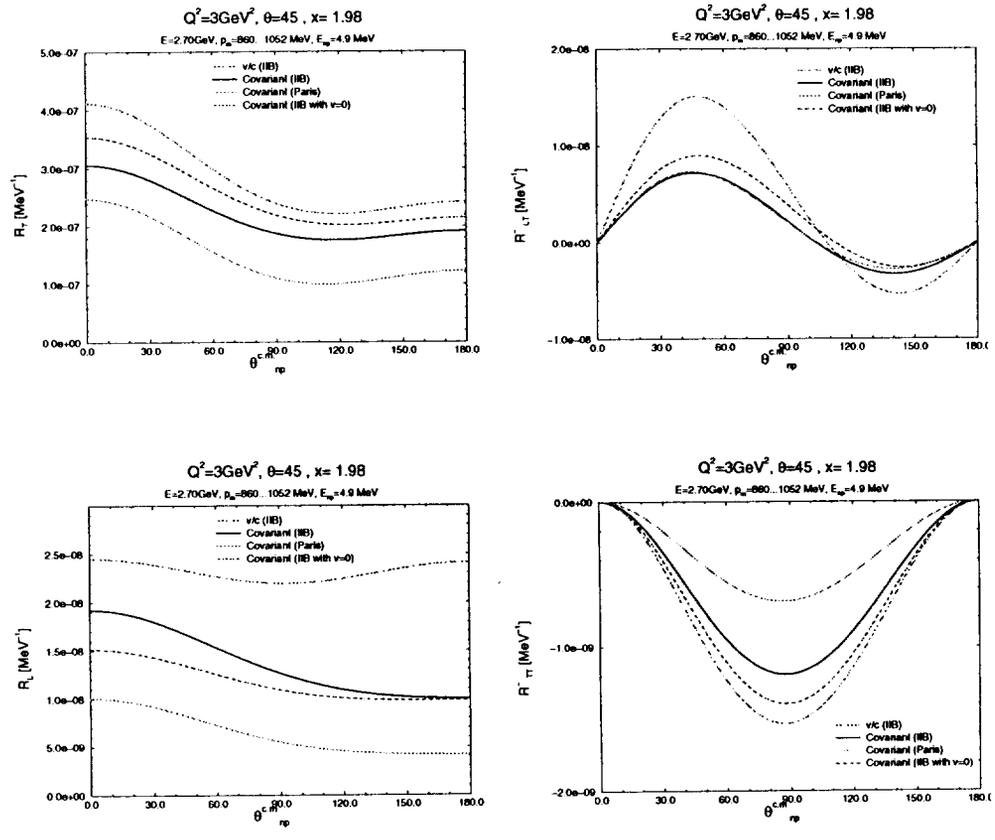

FIG. 17. The four structure functions at "large" Q^2 and small W. All are sensitive to *all* effects.

ACKNOWLEDGMENTS

This work was supported in part by the DOE under grant Number DE-FG02-97ER41032.

---

[1] B. D. Keister and W. N. Polyzou, *Adv. Nucl. Phys.* **20**, 225 (1991). See also the *Round Table Discussion* by F. Coester *et al*, in the Proceedings of the Trieste Conference (1995), and the discussion lead by J. A. Tjon and F. Lev, *Proceedings of the XVth European Conference on Few Body Problems in Physics*, eds. R. Guardiola and V. Vento, Few-Body Systems **8** (1995).
[2] J. Fleisher and J. A. Tjon, Nucl. Physics. **B84**, 375 (1975); Phys. Rev. D **15**, 2537 (1977); D **21**, 87 (1980)
[3] E. E. Salpeter, Phys. Rev. **87**, 328 (1952).
[4] R. Blankenbecler and R. Sugar, Phys. Rev. **142**, 1051 (1966).
[5] S. J. Wallace and V. B. Mandelzweig, Nucl. Phys. **A503**, 673 (1989).
[6] F. Gross, Phys. Rev. **186**, 1448 (1969); Phys. Rev. D **10**, 223 (1974); C **26**, 2203 (1982).
[7] F. Gross, J. W. Van Orden, and K. Holinde, Phys. Rev. C **45**, 2094 (1992).
[8] A. Stadler and F. Gross, Phys. Rev. Lett. **78**, 26 (1997).
[9] W. W. Buck and F. Gross, Phys. Rev. D **20**, 2361 (1979).
[10] F. Gross, Phys. Rev. C **26**, 2226 (1982).
[11] F. Gross, lectures at the University of Hannover (1982), unpublished.
[12] A. Stadler, F. Gross, and M. Frank, Phys. Rev. C**56**, 2396 (1997).
[13] J. W. Van Orden, N. Devine, and F. Gross, Phys. Rev. Letters **75**, 4369 (1995).
[14] F. Gross and D. O. Riska, Phys. Rev. C **36**, 1928 (1987).
[15] R. Arnold, C. Carlson, and F. Gross, Phys. Rev. C **21**, 1426 (1980).
[16] E. Hummel and J. A. Tjon, Phys. Rev. Letters **63**, 1788 (1989); Phys. Rev. C**42**,423 (1990).
[17] F. Gross, in *Proceedings ot the 6th International Conference on Few Body Problems*, Quebec City, ed. by R. J. Slobodrian *et al* (Univ. of Laval Press, Quebec, 1975), p. 782.
[18] P. Mergell, Ulf-G. Meissner, and D. Drechsel, Nucl. Phys. A**596**, 367 (1996).
[19] K. L. Mitchell, Ph.D. thesis, Kent State University, 1995 (unpublished);
K. L. Mitchell and P. C. Tandy, private communication
[20] H. Ito and F. Gross, Phys. Rev. Letters **71**, 2555 (1993).
[21] R. Schiavilla and D. O. Riska, Phys. Rev. C **43**, 437 (1991).
[22] J. Tjon, Few-Body Sys. Suppl, **5**, 5 (1992).

[23] G. Beck and H. Arenhövel, Few-Body Sys. **13**, 165 (1992);
T. Wilbois, G. Beck and H. Arenhövel, Few-Body Sys. **15**, 39 (1993);
G. Beck, T. Wilbois, and H. Arenhövel, Few-Body Sys. **17**, 91 (1994).
[24] J. Adam, F. Gross, P. Ulmer, and J. W. Van Orden, in preparation.
[25] V. Dmitrašinović and Franz Gross, Phys. Rev. C **40**, 2479 (1989); Phys. Rev. C **43**, 1495(E) (1991).
[26] H. Arenhövel, W. Leidemann, E.L. Tomusiak, Few-Body Systems **15**, 109 (1993).
[27] M. Bernheim, et. al., Nucl.Phys. **A365**, 349 (1981).